JEE Journal of Ecological Engineering

Journal of Ecological Engineering, 2026, 27(6), 30–41
https://doi.org/10.12911/22998993/215938
ISSN 2299–8993, License CC-BY 4.0

Received: 2025.12.07
Accepted: 2026.04.16
Published: 2026.05.01

Enhancing thermomechanical stability and environmental degradability of chitosan-starch composite films using extra virgin olive oil

Muhammad Hasan[1*], Dinia Astira[2], Rusman[1], Said Ali Akbar[3], Uswatun Hasanah[4]

[1] Department of Chemistry Education, Universitas Syiah Kuala Darussalam, Banda Aceh 23111, Indonesia
[2] Department of Chemistry, Faculty of Science and Data Analytics, Institut Teknologi Sepuluh Nopember, Sukolilo, Surabaya 60111, Indonesia
[3] Department of Aquaculture, Faculty of Marine and Fisheries, Universitas Syiah Kuala, Banda Aceh 23111, Indonesia
[4] Department of Geophysical Engineering, Universitas Syiah Kuala, Darussalam Banda Aceh, 23311 Indonesia
* Corresponding author's e-mail: muhammadhasan.kimia@usk.ac.id

ABSTRACT

This study investigates the physicochemical, functional, and biodegradation properties of chitosan-sago starch (CHSS) films incorporated with extra virgin olive oil (EVOO) as a natural bioactive additive. Films containing 0–5% EVOO were characterized using FTIR, XRD, mechanical testing, water uptake analysis, water vapor transmission measurements, TGA–DTG–DSC, antioxidant assays, and soil burial degradation. FTIR confirmed that EVOO did not introduce new chemical bonds but modified the hydrogen-bonding environment of the matrix, while XRD revealed reduced crystallinity with increasing EVOO content. Mechanical properties showed no statistically significant differences among treatments, indicating that EVOO did not compromise film strength or flexibility within the tested range. EVOO increased water uptake due to matrix relaxation yet decreased WVTR and WVP, suggesting simultaneous enhancement of hydrophilic absorption and moisture-barrier resistance. Thermal analyses showed typical three-stage degradation with slight stability improvements at moderate EVOO levels. Antioxidant activity improved significantly with higher EVOO concentrations (from 45.3% to 65.4%), with CHSS5 exhibiting the highest DPPH radical scavenging activity. All films remained highly biodegradable, achieving more than 70% weight loss after 20 days of soil burial. Overall, EVOO incorporation enhanced the functional performance of CHSS films, particularly antioxidant capacity and water vapor barrier properties while maintaining biodegradability, demonstrating strong potential for sustainable active food packaging applications.

Keywords: biodegradable films, chitosan, sago starch, extra virgin olive oil, sustainable packaging, biodegradation.

INTRODUCTION

The growing environmental concerns associated with synthetic plastic waste have led to an urgent need for sustainable alternatives in packaging applications. Conventional petroleum-based plastics contribute significantly to pollution and are persistent in the environment due to their non-biodegradable nature (Hasan et al., 2024). As a response, biopolymer-based films have gained increasing attention as eco-friendly materials that offer biodegradability while maintaining essential packaging properties (Hasan et al., 2023). Chitosan and sago starch (CH/SS) have emerged as promising biopolymers for the development of biodegradable films due to their natural abundance, biocompatibility, and excellent film-forming properties (Lau et al., 2024). Chitosan, a derivative of chitin, possesses antimicrobial and antioxidant activities, while sago starch provides good mechanical strength and flexibility. However, pure CH/SS films exhibit limitations in water barrier properties and susceptibility to environmental

degradation, which restrict their practical applications in food and biomedical packaging (Gamage et al., 2024).

To address these challenges, the incorporation of hydrophobic agents, such as extra virgin olive oil (EVOO), has been explored as a potential strategy to enhance the functional properties of biopolymer films. EVOO is rich in bioactive compounds, including polyphenols and tocopherols, which contribute to improved antioxidant properties and increased hydrophobicity (Hasan et al., 2020). Recent studies have demonstrated that the addition of active compounds, such as plant extracts, essential oils, and phenolic compounds, into biopolymer matrices significantly improves their functional properties (Gunal-Koroglu and Capanoglu, 2024). For instance, the incorporation of lemongrass essential oil into cassava starch-based films enhanced their antioxidant and antimicrobial properties while improving the water resistance of the films (Istiqomah et al., 2022). Similarly, the integration of rambutan peel extract into cassava starch-whey protein films resulted in improved moisture barrier properties and increased antioxidant activity, further demonstrating the effectiveness of bioactive additives in enhancing biopolymer-based films (Chollakup et al., 2020). (Othman et al., 2024) also reported that chitosan-starch composite films containing active agents, such as phenolic extracts, exhibited enhanced thermal stability and antimicrobial properties, emphasizing their multifunctional applications. Despite extensive studies on chitosan–starch films incorporating lipids or vegetable oils, most reports focus on commonly used starch sources and emphasize isolated property enhancements rather than integrated functional and environmental performance. In addition, limited attention has been given to understanding how hydrophobic additives such as extra virgin olive oil influence structure–property–biodegradation relationships in chitosan–sago starch systems. Compared to our previous studies focusing on chitosan-based composite films, this work extends the investigation toward EVOO-modified chitosan–sago starch systems with an emphasis on integrated functional and environmental performance. Therefore, this study aims to develop and comprehensively characterize biodegradable chitosan-sago starch composite films incorporated with EVOO, and to evaluate the effects of EVOO on their structural, mechanical, barrier, thermal, antioxidant, and biodegradation properties.

MATERIAL AND METHODS

Materials

Native sago starch powder was obtained from Sago Aren Co., Ltd. (Indonesia). Extra virgin olive oil (EVOO) was sourced from Gautama Indah Perkasa Co., Ltd. (Jakarta, Indonesia). Blue crab shell-derived chitosan powder (particle size: 200–300 mesh; molecular weight: 102 kDa; degree of deacetylation: 96.24%) was supplied by Chimultiguna Co., Ltd. (Indramayu, Indonesia). Meanwhile, 2,2-diphenyl-1-picrylhydrazyl, glycerol, and glacial acetic acid were procured from Sigma Aldrich (Darmstadt, Germany).

Preparation of chitosan/sago starch (CH/SS) biofilms

CH/SS biofilms were prepared by the solvent casting method following (Hiremani et al., 2021), with slight modifications. Chitosan (2% w/v) was dissolved in 1% acetic acid under stirring for 24 h, while sago starch (3% w/v) was gelatinized in distilled water at 80 °C for 30 min. The two solutions were mixed at a 1:1 ratio, and glycerol (30% w/w, based on total polymer weight) was added as a plasticizer. The mixture was homogenized at 10.000 rpm for 5 min, followed by the incorporation of EVOO at 0, 1, 2, and 5% (w/w). The resulting solutions were cast into petri dishes, dried at 40 °C for 48 h, and conditioned at 50% relative humidity for 48 h prior to characterization

Fourier transform infrared spectroscopy (FTIR) analysis

The chemical structure of the films was analyzed using a Cary 630 FTIR spectrometer in transmission mode. Each film sample was cut into small sections (approximately 1 × 1 cm) and placed directly in the sample holder for measurement. The spectra were recorded over the wavenumber range of 4000–400 cm^{-1}, with a spectral resolution of 4 cm^{-1} and 32 scans per sample. Prior to measurement, the background spectrum was collected to eliminate atmospheric interference.

X-ray diffraction analysis

The crystalline structure and molecular ordering of the films were examined using X-ray diffraction (XRD). Diffraction patterns were

recorded using an X-ray diffractometer operating at 40 kV and 30 mA with Cu Kα radiation (λ = 1.5406 Å). Film samples were cut into flat strips and mounted on the sample holder to ensure uniform exposure. Data were collected over a 2θ range of 5–35° at a scan rate of 2°/min. The obtained diffractograms were smoothed and normalized before analysis

Thermal analysis (simultaneous TGA–DSC and DTG calculation)

Thermal behavior of the films was evaluated using a DSC–TGA Linearis STA PT 1600 simultaneous thermal analyzer. Approximately 5–10 mg of each film sample was placed in an alumina crucible and heated from 30 to 600 °C at a constant heating rate of 10 °C/min under a nitrogen atmosphere to prevent oxidative degradation. The instrument simultaneously recorded thermogravimetric (TGA) and differential scanning calorimetry (DSC) signals. The derivative thermogravimetric (DTG) curves were obtained by numerically differentiating the TGA data. From these thermal profiles, Tonset, Tmax, Tend, major decomposition stages, and residual mass were determined to assess the thermal stability of the EVOO-modified CH/SS films.

Mechanical properties analysis (tensile strength and elongation at break)

The mechanical properties of the films were evaluated using an IK Tester MCT-2150 apparatus following the ASTM D638 standard. Film samples were cut into dumbbell-shaped specimens with dimensions specified by the standard, and each specimen was conditioned at 25 °C and 50% relative humidity for 24 hours prior to testing. Tensile strength (TS) and elongation at break (EB) were measured at a crosshead speed of 5 mm/min. At least three replicates were tested for each formulation. The obtained stress–strain curves were used to calculate TS and EB, and the results were expressed as mean ± standard deviation.

Water uptake

The water uptake of the films was measured by immersing them in distilled water for 10, 20, 30, and 40 seconds, following the procedure described by (Iyuke et al., 2023), with minor adjustments. The films were blotted with filter paper, and the weight gain was recorded. Water uptake (%) was calculated as:

$$Water\ uptake\ (\%) = \frac{W_f - W_i}{W_i} \times 100 \quad (1)$$

where: W_f and W_i are the final and initial weights of the films, respectively.

Water vapor transmission rate (WVTR)

Water vapor transmission rate (WVTR) was determined following the ASTM E96 standard gravimetric method, as described by (Ashfaq et al., 2022), with slight procedural modifications. The films were cut into circular pieces and sealed on the top of test cups containing silica gel. The cups were placed in a desiccator maintained at 75% relative humidity and 25 °C. The weight gain of the cups was recorded at specific time intervals. The WVTR was calculated using the equation:

$$WVTR = \frac{W}{A \times t} \quad (2)$$

where: W is the weight gain (g), A is the film area (m²), and t is the time (h).

Water vapor permeability

Water vapor permeability (WVP) was determined using the gravimetric method, as described by (Hasan et al., 2023), with minor adjustments to suit the experimental setup. The films were mounted on test cups containing silica gel, sealed, and stored in a desiccator at 75% relative humidity. The weight gain was recorded at intervals, and WVP was calculated using the following equation:

$$WVP = \frac{W \times x}{A \times t \times \Delta P} \quad (3)$$

where: W is the weight gain (g), x is the film thickness (m), A is the permeation area (m²), t is time (h), and ΔP is the partial vapor pressure difference (Pa).

Antioxidant activity

The antioxidant activity of the films was evaluated using the DPPH radical scavenging assay, as described by (Vostrejs et al., 2020), with minor modifications. Film extracts were prepared by dissolving 0.1 g of film in 10 mL of methanol. The extracts (1 mL) were mixed with 2 mL of 0.1 mM DPPH solution and incubated in the dark

for 30 minutes. The absorbance was measured at 517 nm using a UV-Vis spectrophotometer. The percentage of DPPH scavenging activity was calculated using:

$$DPPH\ (\%) = \frac{A_c - A_s}{A_c} \times 100 \qquad (4)$$

where: A_c is the control absorbance and A_s is the sample absorbance.

Biodegradation study

The biodegradation of the films was assessed through a soil burial test, following the method outlined by (Wattanawong and Aht-Ong, 2021), with minor modifications to align with the experimental conditions. Film samples (2 × 2 cm) were buried in compost at 60% moisture content and incubated at room temperature. The weight loss was recorded at intervals of 5, 10, 15, and 20 days to determine the degradation rate.

Statistical analysis

All experiments were performed in triplicate, and results were expressed as mean ± standard deviation. One-way ANOVA was conducted to evaluate significant differences among groups. Tukey's post-hoc test was subsequently applied for multiple comparisons at a significance level of $p < 0.05$.

RESULT AND DISCUSSION

Chemical structure characterization

The FTIR spectra of CHSS0, CHSS1, CHSS2, and CHSS5 films (Figure 1a) reveal the characteristic functional groups of the chitosan–sago starch matrix and the structural modifications induced by EVOO incorporation. All samples exhibited a broad absorption band centered around 3300 cm^{-1}, corresponding to the overlapping O–H and N–H stretching vibrations (Arcana et al., 2010), which originate from hydroxyl groups of starch and chitosan as well as amino groups of chitosan. The slight decrease in intensity of this band with increasing EVOO concentration suggests a reduction in hydrogen bond density, likely due to partial replacement of polymer–polymer interactions by polymer–lipid interactions (Kittur et al., 2002).

A distinct peak around 2900 cm^{-1} was observed for all films, attributed to C–H stretching of aliphatic chains. This band becomes slightly more pronounced in EVOO-containing films, consistent with the presence of long-chain fatty acids in EVOO that introduce additional alkyl stretching contributions (Hasan et al., 2020). The region near 1550 cm^{-1}, corresponding to amide II vibrations (N–H bending coupled with C–N stretching), remained present across all samples, confirming the structural integrity of chitosan's amide functionalities (Borges et al., 2019). Minor shifts in this band in EVOO-loaded films indicate weak interactions between chitosan and lipid components, likely arising from hydrophobic–hydrophilic microphase reorganization (Kishimoto, 2021).

The absorption band at approximately 1000 cm^{-1}, assigned to C–O–C stretching of glycosidic linkages in starch and chitosan, persisted in all formulations. A gradual decrease in intensity with increasing EVOO concentration suggests a subtle alteration in the polysaccharide network, potentially due to decreased crystallinity or increased molecular mobility induced by the lipid phase (Ferreira et al., 2021). Overall, the FTIR results demonstrate that EVOO incorporation does not

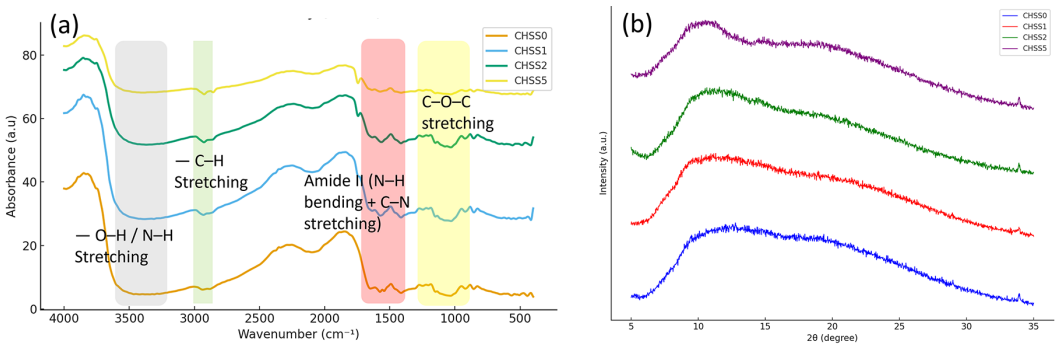

Figure 1. (a) FTIR spectra showing characteristic functional groups and (b) XRD patterns illustrating structural features of CHSS films incorporated with varying concentrations of EVOO

introduce new functional groups, confirming the absence of chemical reactions between components. Instead, EVOO induces physical interactions primarily through hydrogen bond disruption and hydrophobic association – which collectively influence the structural arrangement of the biopolymer matrix. These spectral changes correlate well with observed variations in mechanical, barrier, and thermal properties reported in subsequent sections.

Structural ordering and crystallinity evolution

The XRD patterns of CHSS0, CHSS1, CHSS2, and CHSS5 films (Figure 1b) reveal the partially crystalline nature of the chitosan–sago starch matrix and the structural modifications induced by EVOO incorporation. All samples displayed a broad diffraction halo centered around $2\theta = 18–22°$, which is characteristic of the semi-crystalline polysaccharide network formed by intermolecular hydrogen bonding among chitosan and starch chains (Tan et al., 2022). This diffuse peak is typically associated with the amorphous–crystalline transition zone of biopolymer films (Kovtun et al., 2024). For the control sample (CHSS0), the broad halo is relatively more pronounced, indicating a moderate degree of structural ordering within the matrix (Bajer et al., 2020). As EVOO concentration increased, a consistent decrease in peak intensity and slight broadening of the halo were observed, particularly in CHSS2 and CHSS5. These changes suggest a reduction in crystallinity, likely caused by interference of lipid molecules with the alignment of polysaccharide chains, thereby disrupting intermolecular packing (Esfandiari et al., 2025).

The hydrophobic triglycerides and fatty acids present in EVOO may act as spacing agents, reducing the extent of chain–chain association and producing a more amorphous structure. This aligns with FTIR observations indicating weakened hydrogen bonding in EVOO-containing films. The decreased structural ordering is also consistent with the enhanced flexibility and decreased tensile strength seen in mechanical testing. No new crystalline peaks appeared upon the addition of EVOO, confirming that the lipid does not crystallize into detectable domains within the matrix and remains molecularly dispersed or forms amorphous microphases (Wang et al., 2025). The overall trend of reduced crystallinity with increasing EVOO is typical for polymer–lipid composite films and has been reported widely for chitosan-based bioplastics (Esfandiari et al., 2025; Hasan et al., 2025). Taken together, the XRD analysis demonstrates that EVOO incorporation leads to a progressive amorphization of the film structure, which contributes to the observed changes in barrier behavior, water uptake, and thermal properties discussed in subsequent sections (Wang et al., 2025).

Mechanical behavior of the films

The mechanical properties of the CHSS films were evaluated through tensile strength (TS) and elongation at break (EB) measurements (Figure 2). The control film (CHSS0) exhibited the highest TS, reflecting the intrinsic strength of the chitosan–sago starch matrix reinforced by extensive hydrogen bonding and semi-crystalline domains (Hermawan et al., 2019). Upon incorporation of EVOO, a noticeable decline in TS was observed across all modified films (CHSS1–CHSS5), with

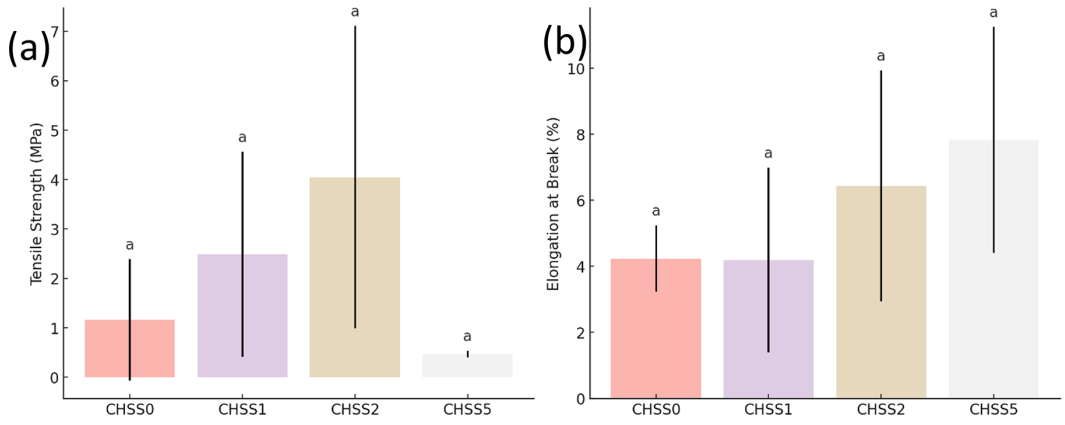

Figure 2. Mechanical properties, (a) tensile strength and (b) elongation at break of CHSS0, CHSS1, CHSS2, and CHSS5. note: Different letters above the bars indicate statistical groupings based on Tukey's HSD test ($p < 0.05$)

CHSS5 showing the lowest value. This progressive reduction can be attributed to the plasticizing and matrix-disrupting effects of EVOO, which interferes with polysaccharide–polysaccharide interactions and reduces molecular packing efficiency (Devi et al., 2024) , as supported by the FTIR and XRD analyses.

In contrast to TS, the EB values increased with higher EVOO content, indicating enhanced ductility. EVOO, which contains long-chain triglycerides and unsaturated fatty acids, acts primarily as a natural plasticizer, increasing polymer chain mobility and reducing brittleness (Khalil et al., 2019; Souto et al., 2021). The CHSS5 film exhibited the highest EB, consistent with a more flexible and less ordered polymer network. This inverse relationship between TS and EB is characteristic of films in which lipid components disrupt the original hydrogen-bonded network of chitosan and starch (Wibowo et al., 2023). Statistical analysis using Tukey HSD ($p > 0.05$) indicated that the differences among treatments were not statistically significant, with CHSS0 distinct from all EVOO-containing films in both TS and EB measurements. The absence of statistically significant changes in tensile strength and elongation at break indicates that EVOO incorporation does not compromise the mechanical integrity of CHSS films, while still enabling functional enhancements critical for active and biodegradable packaging applications. The intermediate samples (CHSS1 and CHSS2) showed transitional values, reflecting partial modification of the polymer matrix, whereas CHSS5 represented the most pronounced plasticization effect. These mechanical trends corroborate structural findings from FTIR and XRD, indicating that EVOO incorporation induces a shift toward a more amorphous, flexible system. Overall, the mechanical data demonstrate that EVOO effectively modulates the strength–flexibility balance of the films. While higher EVOO levels reduce tensile strength, they substantially enhance ductility, offering tunable mechanical performance for specific packaging applications where flexibility is desirable.

Water uptake and water vapor permeability (WVTR and WVP)

The water uptake behavior of the films is presented in Figures 3a–b. All samples exhibited a rapid increase in water absorption during the first 10 seconds, which is typical for polysaccharide-based films due to the abundance of hydrophilic –OH groups. After this initial phase, the rate of absorption gradually decreased and approached a plateau. The control film (CHSS0) displayed the lowest water uptake (~12%), whereas the incorporation of EVOO progressively increased water absorption, with the highest values observed for CHSS5 (~18–20%). This trend is associated with the increased structural heterogeneity caused by dispersed oil droplets, which introduce microvoids within the chitosan–starch matrix and thereby facilitate water diffusion (Khalil et al., 2019). As shown by the Tukey HSD analysis (Figure 4b), CHSS5 differed significantly from CHSS0 ($p < 0.05$), while CHSS1 and CHSS2 fell into overlapping statistical groups, indicating that the effect of EVOO becomes more pronounced only at higher concentrations.

Water vapor transmission properties are shown in Figures 4a–b. The WVTR values decreased consistently from CHSS0 to CHSS5, demonstrating that EVOO acts as a hydrophobic

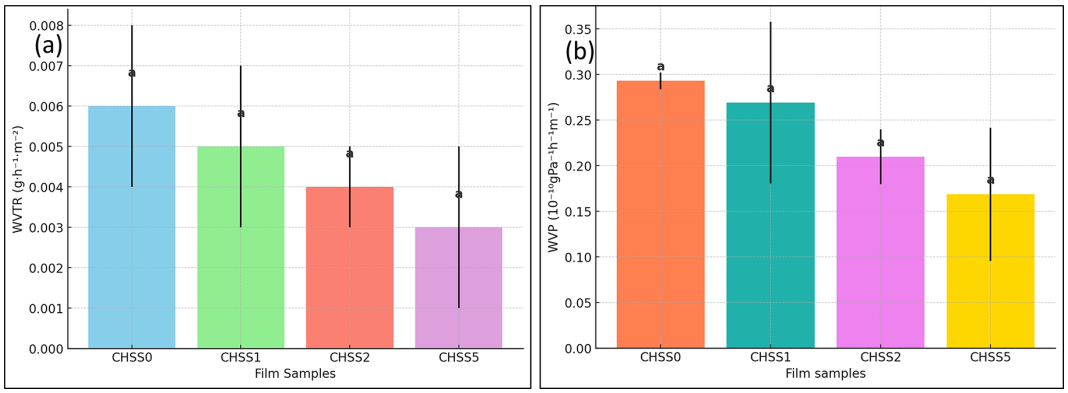

Figure 3. (a) Water vapor transmission rate (WVTR) of CHSS0, CHSS1, CHSS2, and CHSS5 films, (b) water vapor permeability (WVP) of the films. Different letters above the bars denote significant differences among samples (Tukey, $p < 0.05$)

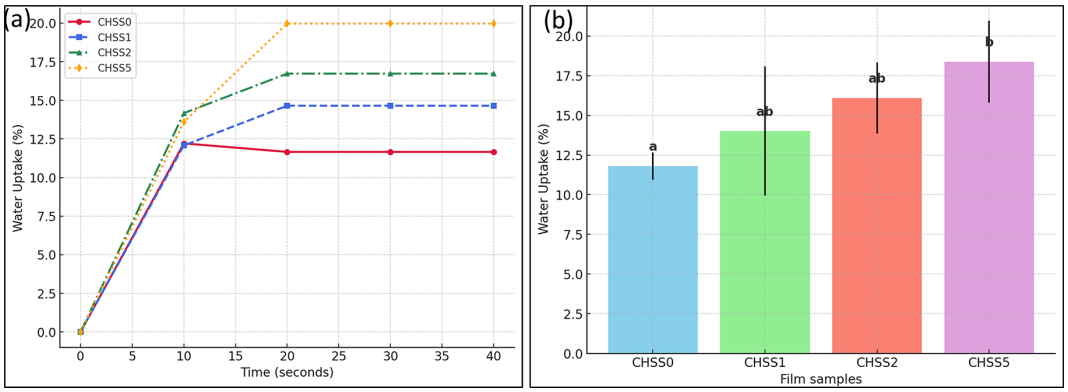

Figure 4. (a) Water uptake profiles of CHSS0, CHSS1, CHSS2, and CHSS5 films, (b) average water uptake (%) of the films after reaching equilibrium, with error bars representing standard deviations and different letters indicating statistically significant differences (Tukey, $p < 0.05$)

phase capable of hindering water vapor migration through a tortuosity barrier mechanism (Liyanapathiranage et al., 2023). In the control film, vapor molecules diffuse relatively freely through the continuous hydrophilic matrix. However, the presence of oil droplets disrupts this continuity, forcing water vapor to navigate more complex and winding pathways, thereby reducing flux (Esfandiari et al., 2025). A similar trend is observed for WVP: CHSS0 exhibited the highest permeability, followed by CHSS1 and CHSS2, while CHSS5 showed the lowest value. Overall, increasing EVOO content enhances the film's moisture barrier efficiency.

Statistical analysis of WVP (Figure 4b) further reveals that only CHSS0 differs significantly from the EVOO-containing films ($p < 0.05$), whereas the differences among CHSS1, CHSS2, and CHSS5 were not statistically significant. This suggests that although EVOO improves water vapor barrier properties, incremental increases beyond 1–2% do not produce sufficiently large changes to be statistically distinguishable at the 95% confidence level. Taken together, these results show that EVOO exerts a dual influence: (i) it increases water uptake due to the generation of microstructural voids that enhance short-term water absorption, while (ii) simultaneously decreasing water vapor permeability as the hydrophobic oil droplets create a more tortuous diffusion pathway. This combination results in a unique mass transport profile characteristic of lipid-modified biopolymer films.

Thermal properties

The thermal degradation profiles of the films are presented in Figure 5a–b. All samples exhibited a characteristic three-stage decomposition pattern typical of chitosan–starch systems. The initial mass loss occurring below 120 °C corresponds to the evaporation of free and bound water, reflecting the hydrophilicity of the polysaccharide matrix (Rachmina et al., 2024). Films containing EVOO (CHSS1–CHSS5) showed slightly lower moisture-related loss compared to the control sample (CHSS0), indicating reduced water affinity due to the hydrophobic nature of the oil phase. The major degradation event was observed between 230 and 320 °C, as shown by the prominent DTG peaks (Figure 5b). This region is associated with the depolymerization of chitosan and starch backbones, including cleavage of glycosidic linkages and decomposition of the polysaccharide structures (Hasan et al., 2025). The DTG_max values for CHSS1 and CHSS2 shifted marginally toward higher temperatures relative to CHSS0, suggesting a slight improvement in thermal stability. This enhancement is likely attributed to EVOO acting as a physical barrier that slows heat transfer and inhibits chain mobility (Giannakas et al., 2017). However, at higher EVOO concentration (CHSS5), the DTG peak returned closer to that of the control film, implying that excessive oil disrupts polymer–polymer interactions and weakens the structural cohesion of the matrix (Devi et al., 2024). A final degradation region (>450 °C) corresponds to the decomposition of carbonaceous char. Samples containing EVOO produced slightly higher residual mass at 600 °C compared to CHSS0, indicating enhanced char formation. The hydrophobic EVOO domains may promote localized carbonization during high-temperature treatment, contributing to improved thermal resistance (Mbonambi et al., 2025).

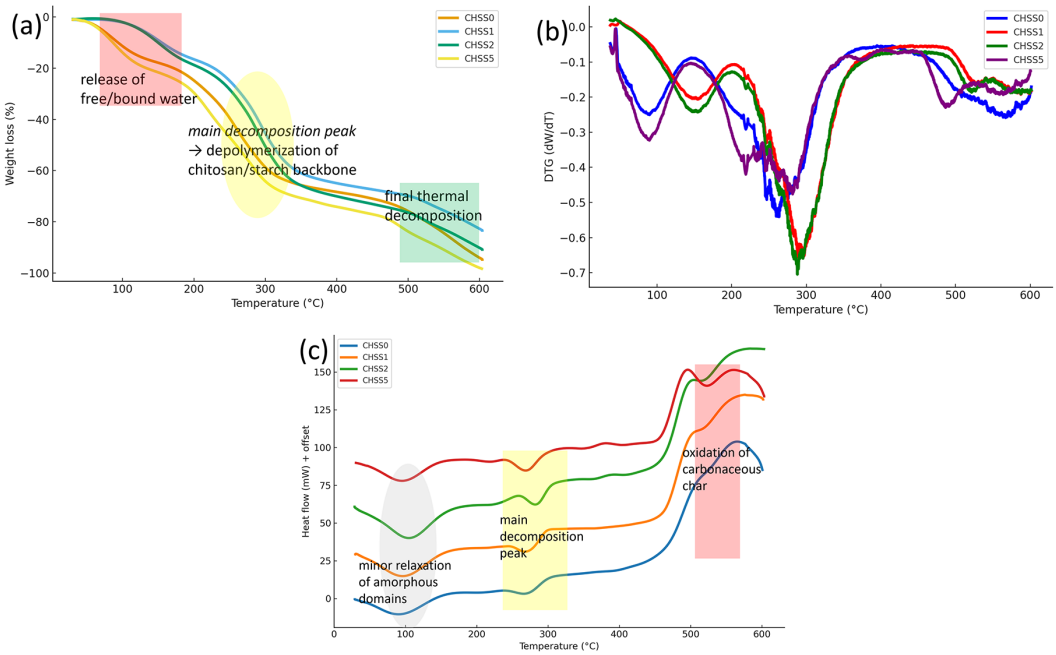

Figure 5. (a) TGA curves of CHSS0, CHSS1, CHSS2, and CHSS5 films, (b) DTG profiles highlighting differences in decomposition rates, (c) DSC thermograms

Figure 5c shows the DSC thermograms, which further support the observations from TGA. The first endothermic transition around 80–100 °C corresponds to water loss and relaxation of amorphous domains. A broad thermal event between 250 and 300 °C represents the main decomposition peak of the chitosan–starch network, consistent with the DTG analysis (Javaid et al., 2020). Films containing EVOO exhibited subtle shifts in peak intensity and onset temperature, suggesting that the oil modifies chain mobility and microstructural packing (Hasan et al., 2024). Notably, a high-temperature exothermic region (480–550 °C) appeared more pronounced in EVOO-containing samples, attributed to oxidation of carbonaceous residues. Overall, the combined TGA, DTG, and DSC results indicate that moderate EVOO incorporation (1–2%) slightly enhances thermal stability by reinforcing char formation and increasing the energy required for degradation (Shamsuri and Md. Jamil, 2020). However, at higher loading (5%), the discontinuity introduced by large oil domains weakens structural integrity, reducing the stabilizing effect. These findings highlight the importance of balancing EVOO concentration to optimize both thermal and functional properties of the biocomposite film.

Antioxidant activity

Figure 6 illustrates the antioxidant activity of CH/SS films as a function of EVOO concentration. Antioxidant properties play a crucial role in extending the shelf life of food products by inhibiting oxidative degradation. EVOO is known to be rich in bioactive compounds such as polyphenols and tocopherols, which can significantly enhance the antioxidant activity of biopolymer films (Hossen et al., 2024). The results indicate a progressive increase in antioxidant activity with increasing EVOO content. CHSS0 exhibited the lowest antioxidant capacity, whereas CHSS5 demonstrated the highest activity. This trend suggests that EVOO effectively incorporated its bioactive components into the CH/SS matrix, contributing to the radical scavenging ability of the films (Lafeuillee and Maharaj, 2025). Statistical analysis further confirms significant differences between the formulations, with CHSS5 showing a marked improvement compared to the control (CHSS0).

The correlation between antioxidant activity and EVOO concentration highlights the potential of these biofilms for active packaging applications. Films with higher antioxidant properties can help protect food products from oxidative deterioration, thereby extending their shelf life (Zhu et al., 2023). However, the homogeneity of EVOO dispersion within the polymer matrix should be considered

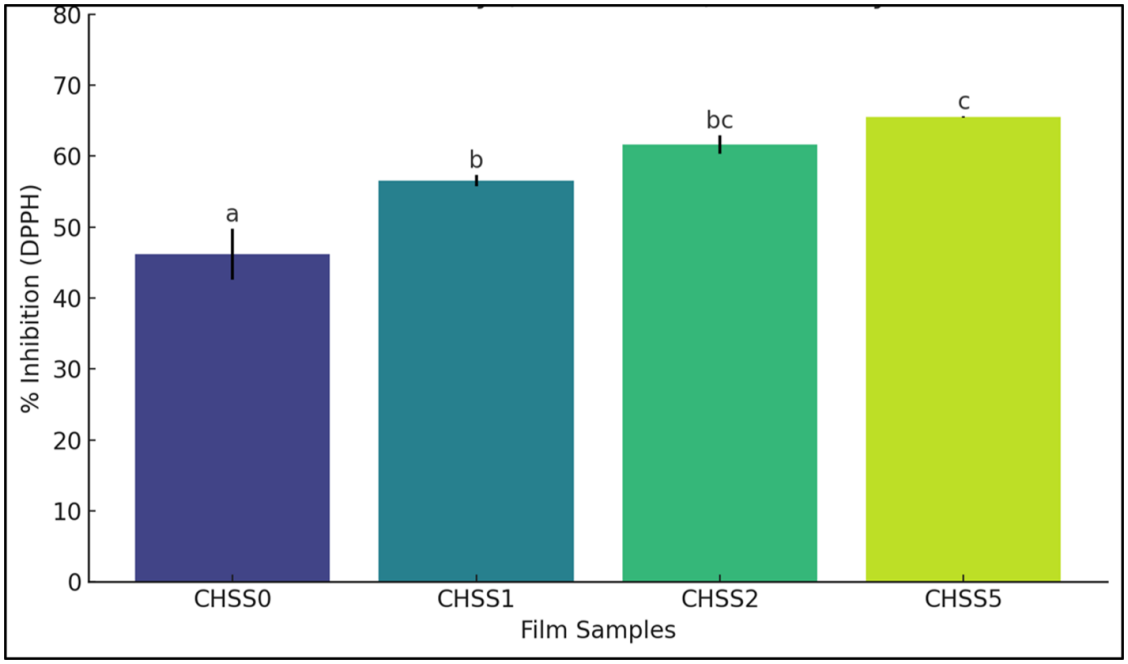

Figure 6. Antioxidant activity of films. Different letters above the bars indicate statistically significant differences among samples according to Tukey's HSD test ($p < 0.05$)

to ensure consistent antioxidant performance throughout the film. These findings underscore the multifunctional role of EVOO in CH/SS biofilms, providing both moisture barrier enhancement and antioxidant activity (Wang et al., 2022).

Biodegradation behavior

The biodegradation behavior of the films under soil burial conditions is presented in Figure 7a–b. Visual observations (Figure 7a) show a progressive deterioration of all samples over the 20-day burial period. During the first 5 days, the films primarily exhibited surface softening and increased opacity, reflecting the initial microbial colonization and moisture penetration into the polysaccharide matrix (Arooj et al., 2024). By day 10, the structural integrity of the films was visibly reduced, with fragmentation becoming evident, especially in CHSS0, CHSS1, and CHSS2. After 15–20 days, all films were substantially degraded, with only irregular fragments remaining and pronounced darkening due to soil–microbe interaction. The quantitative weight-loss data (Figure 7b) closely align with the visual degradation trend. All films showed a rapid degradation phase during the first 5 days, losing approximately 50% of their initial mass, an expected behavior for

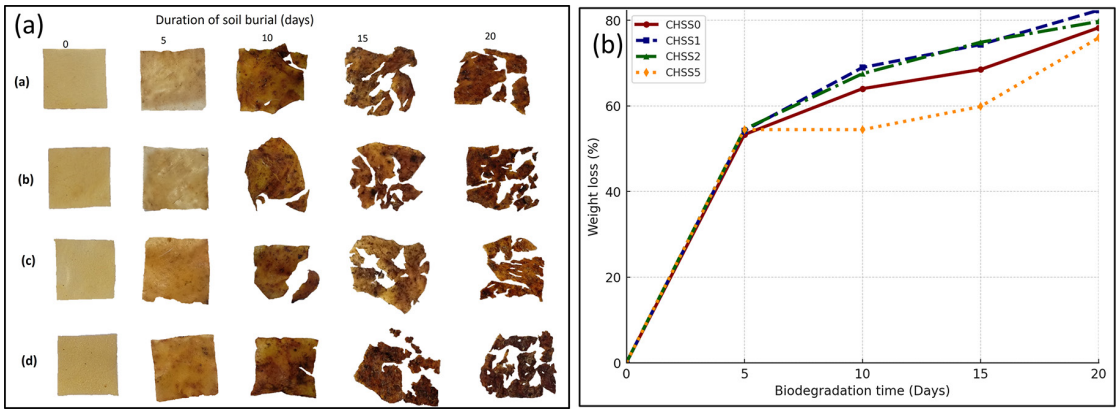

Figure 7. (a) Visual degradation of CHSS0, CHSS1, CHSS2, and CHSS5 films during soil burial for 0–20 days. (b) weight loss (%) of the films during soil burial biodegradation

hydrophilic biopolymer films that readily absorb water and are susceptible to enzymatic hydrolysis (Tan et al., 2022). Beyond day 10, the degradation rate continued but gradually slowed as the remaining fragments became smaller and less accessible to microorganisms.

Interestingly, the EVOO-modified films demonstrated slightly different biodegradation profiles. CHSS0, CHSS1, and CHSS2 exhibited similar weight-loss patterns, with final degradation values approaching 75–80% by day 20. In contrast, CHSS5 showed a noticeably lower degradation rate during the mid-phase (days 5–15), likely due to the higher hydrophobic component introduced by the 5% EVOO. The dispersed oil droplets can partially shield the polymer matrix from microbial enzymes and moisture, thereby slowing degradation (Gupta et al., 2022). However, by day 20, CHSS5 still reached a substantial total degradation of approximately 70%, confirming that EVOO incorporation does not inhibit biodegradability but merely modulates the degradation kinetics. It should be noted that the 20-day soil burial test provides an early-stage and comparative evaluation of biodegradation behavior rather than a complete long-term degradation profile. In summary, the soil-burial test demonstrates that all films remain fully biodegradable despite the presence of EVOO. The rapid early-stage degradation followed by slower fragmentation is characteristic of polysaccharide-based materials, and the slight retardation observed at higher EVOO levels reflects the predictable influence of hydrophobicity. These results confirm the suitability of the EVOO-modified chitosan–starch films for environmentally responsible applications and highlight their potential as sustainable active packaging materials.

Despite the promising functional and environmental performance of EVOO-modified CHSS films, several limitations should be acknowledged. The biodegradation and antioxidant evaluations were conducted as short-term assessments and did not capture long-term stability under extended storage, light exposure, or temperature variations. In addition, EVOO incorporation primarily acted as a functional structure modifier rather than a mechanical reinforcement agent, which may limit applications requiring high mechanical strength. Furthermore, the present study was performed at laboratory scale, and future work is needed to assess scalability and long-term performance under real-use conditions.

CONCLUSIONS

This study developed chitosan–sago starch (CHSS) films incorporated with extra virgin olive oil (EVOO) as a natural functional additive. Structural analyses confirmed that EVOO modified the molecular organization of the polymer matrix through physical interactions, leading to reduced crystallinity without forming new chemical bonds. Although mechanical properties were not significantly affected, EVOO clearly influenced moisture-related behavior by increasing water uptake while simultaneously reducing WVTR and WVP due to hydrophobic barrier formation. Thermal analysis indicated a typical three-stage degradation with slight improvements in stability at moderate EVOO contents. Importantly, EVOO significantly enhanced the antioxidant activity of the films while maintaining high biodegradability (>70% mass loss within 20 days). Overall, EVOO-modified CHSS films exhibit improved functional performance without compromising structural integrity or environmental degradability, highlighting their potential for sustainable active food packaging applications.

Acknowledgements

The author sincerely acknowledges the financial support provided by the Ministry of Education, Culture, Research, and Technology of the Republic of Indonesia for the research project at Universitas Syiah Kuala.

REFERENCES

1. Arcana, I. M., Bundjali, B., Hasan, M., Hariyawati, K., Mariani, H., Anggraini, S. D., Ardana, A. (2010). Study on properties of poly(urethane-ester) synthesized from prepolymers of ε-Caprolactone and 2,2-Dimethyl-1,3-Propanediol monomers and their biodegradability. *Journal of Polymers and the Environment*, *18*(3). https://doi.org/10.1007/s10924-010-0189-9
2. Arooj, A., Khan, M., Munawar, K. S. (2024). Preparation and physicochemical characterization of starch/pectin and chitosan blend bioplastic films as future food packaging materials. *Journal of Environmental Chemical Engineering*, *12*(1), 111825. https://doi.org/10.1016/j.jece.2023.111825
3. Ashfaq, J., Channa, I. A., Shaikh, A. A., Chandio, A. D., Shah, A. A., Bughio, B., Birmahani, A., Alshehri, S., Ghoneim, M. M. (2022). Gelatin-and papaya-based biodegradable and edible packaging films to counter plastic waste generation. *Materials*, *15*(3). https://doi.org/10.3390/ma15031046

4. Bajer, D., Janczak, K., Bajer, K. (2020). Novel starch/chitosan/aloe vera composites as promising biopackaging materials. *Journal of Polymers and the Environment*, *28*(3), 1021–1039. https://doi.org/10.1007/s10924-020-01661-7
5. Borges, T. H., Serna, A., López, L. C., Lara, L., Nieto, R., Seiquer, I. (2019). Composition and antioxidant properties of spanish extra virgin olive oil regarding cultivar, harvest year and crop stage. *Antioxidants*, *8*(7). https://doi.org/10.3390/antiox8070217
6. Chollakup, R., Pongburoos, S., Boonsong, W., Khanoonkon, N., Kongsin, K., Sothornvit, R., Sukyai, P., Sukatta, U., Harnkarnsujarit, N. (2020). Antioxidant and antibacterial activities of cassava starch and whey protein blend films containing rambutan peel extract and cinnamon oil for active packaging. *Lwt*, *130*(June), 109573. https://doi.org/10.1016/j.lwt.2020.109573
7. Devi, L. S., Jaiswal, A. K., Jaiswal, S. (2024). Lipid incorporated biopolymer based edible films and coatings in food packaging: A review. *Current Research in Food Science*, *8*, 100720. https://doi.org/https://doi.org/10.1016/j.crfs.2024.100720
8. Esfandiari, Z., Hassani, B., Sani, I. K., Talebi, A., Mohammadi, F., Zomorodi, S., Kaveh, M., Assadpour, E., Khodaei, S. M., Eghbaljoo, H., Gholizadeh, H., Sani, M. A., Jafari, S. M. (2025). Characterization of edible films made with plant carbohydrates for food packaging: A comprehensive review. *Carbohydrate Polymer Technologies and Applications*, *11*, 100979. https://doi.org/https://doi.org/10.1016/j.carpta.2025.100979
9. Ferreira, R. R., Souza, A. G., Quispe, Y. M., Rosa, D. S. (2021). Essential oils loaded-chitosan nanocapsules incorporation in biodegradable starch films: A strategy to improve fruits shelf life. *International Journal of Biological Macromolecules*, *188*(August), 628–638. https://doi.org/10.1016/j.ijbiomac.2021.08.046
10. Gamage, A., Thiviya, P., Liyanapathiranage, A., Wasana, M. L. D., Jayakodi, Y., Bandara, A., Manamperi, A., Dassanayake, R. S., Evon, P., Merah, O., Madhujith, T. (2024). Polysaccharide-Based Bioplastics: Eco-Friendly and Sustainable Solutions for Packaging. *Journal of Composites Science*, *8*(10). https://doi.org/10.3390/jcs8100413
11. Giannakas, A., Patsaoura, A., Barkoula, N. M., Ladavos, A. (2017). A novel solution blending method for using olive oil and corn oil as plasticizers in chitosan based organoclay nanocomposites. *Carbohydrate Polymers*, *157*, 550–557. https://doi.org/10.1016/j.carbpol.2016.10.020
12. Gunal-Koroglu, D., Capanoglu, E. (2024). Plant protein-based edible films and the effect of phenolic additives. *Critical Reviews in Food Science and Nutrition*, 1–21. https://doi.org/10.1080/10408398.2024.2328181
13. Gupta, V., Biswas, D., Roy, S. (2022). A comprehensive review of biodegradable polymer-based films and coatings and their food packaging applications. *Materials 15*(17), 5899. https://doi.org/10.3390/ma15175899
14. Hasan, M., Khaldun, I., Zatya, I., Rusman, R., Nasir, M. (2023). Facile fabrication and characterization of an economical active packaging film based on corn starch–chitosan biocomposites incorporated with clove oil. *Journal of Food Measurement and Characterization*, *17*(1), 306–316. https://doi.org/10.1007/s11694-022-01616-7
15. Hasan, M., Rusman, R., Khaldun, I., Ardana, L., Mudatsir, M., Fansuri, H. (2020). Active edible sugar palm starch-chitosan films carrying extra virgin olive oil: Barrier, thermo-mechanical, antioxidant, and antimicrobial properties. *International Journal of Biological Macromolecules*, *163*, 766–775. https://doi.org/10.1016/j.ijbiomac.2020.07.076
16. Hasan, M., Tasya, G., Khaldun, I., Rusman, R., Hasanah, U. (2025). *Eco-friendly bio-nanocomposite films for sustainable packaging*. *26*(4), 301–312.
17. Hasan, M., Utami, A., Purma, R., Syahrial, S., Rahmayani, R. F. I., Zulfadli, Z. (2024). Development of environmentally friendly and intelligent food packaging bio-nanocomposite films. *Ecological Engineering and Environmental Technology*, *25*(3), 155–164. https://doi.org/10.12912/27197050/178388
18. Hermawan, D., Hazwan, C. M., Owolabi, F. A. T., Gopakumar, D. A., Hasan, M., Rizal, S., Sri Aprilla, N. A., Mohamed, A. R., Khalil, H. P. S. A. (2019). Oil palm microfiber-reinforced handsheet-molded thermoplastic green composites for sustainable packaging applications. *Progress in Rubber, Plastics and Recycling Technology*, *35*(4). https://doi.org/10.1177/1477760619861984
19. Hiremani, V. D., Khanapure, S., Gasti, T., Goudar, N., Vootla, S. K., Masti, S. P., Malabadi, R. B., Mudigoudra, B. S., Chougale, R. B. (2021). Preparation and physicochemical assessment of bioactive films based on chitosan and starchy powder of white turmeric rhizomes (*Curcuma Zedoaria*) for green packaging applications. *International Journal of Biological Macromolecules*, *193*(PB), 2192–2201. https://doi.org/10.1016/j.ijbiomac.2021.11.050
20. Hossen, M. A., Shimul, I. M., Sameen, D. E., Rasheed, Z., Dai, J., Li, S., Qin, W., Tang, W., Chen, M., Liu, Y. (2024). Essential oil–loaded biopolymeric particles on food industry and packaging: A review. *International Journal of Biological Macromolecules*, *265*(P1), 130765. https://doi.org/10.1016/j.ijbiomac.2024.130765
21. Istiqomah, A., Prasetyo, W. E., Firdaus, M., Kusumaningsih, T. (2022). Valorisation of lemongrass essential oils onto chitosan-starch film for sustainable active packaging: Greatly enhanced antibacterial and antioxidant activity. *International Journal of Biological Macromolecules*, *210*, 669–681. https://doi.org/10.1016/j.ijbiomac.2022.04.223
22. Iyuke, S. E., Malaka, J., Maphosa, M., Masubelele, K., Taigbenu, A., Ohimor, E. O. (2023). Fabrication and characterisation of proton exchange membrane from sulfonated natural rubber for possible use as an alternative separator in AGM battery. *Results in Materials*, *17*, 100371. https://doi.org/10.1016/j.rinma.2023.100371

23. Javaid, M. A., Zia, K. M., Zafar, K., Khosa, M. K., Akram, N., Ajmal, M., Imran, M., Iqbal, M. N. (2020). Synthesis and molecular characterization of chitosan/starch blends based polyurethanes. *International Journal of Biological Macromolecules*, *146*, 243–252. https://doi.org/10.1016/j.ijbiomac.2019.12.234
24. Khalil, H. P. S. A., Yap, S. W., Owolabi, F. A. T., Haafiz, M. K. M., Fazita, M. R., Gopakumar, D. A., Hasan, M., Rizal, S. (2019). Techno-functional properties of edible packaging films at different polysaccharide blends. *Journal of Physical Science*, *30*. https://doi.org/10.21315/jps2019.30.s1.2
25. Kishimoto, N. (2021). Light protection performance of wrapping films to prevent the photo-oxidation of extra virgin olive oil during storage in glass bottles. *AIMS Agriculture and Food*, *6*(3), 786–796. https://doi.org/10.3934/agrfood.2021047
26. Kittur, F., Keelara Veerappa, H. P., Kadimi, U., Tharanathan, R. N. (2002). Characterization of chitin, chitosan and their carboxymethyl derivatives by differential scanning calorimetry. *Carbohydrate Polymers*, *49*, 185–193. https://doi.org/10.1016/S0144-8617(01)00320-4
27. Kovtun, G., Casas, D., Cuberes, T. (2024). Influence of glycerol on the surface morphology and crystallinity of polyvinyl alcohol films. In *Polymers 16*(17), 2421. https://doi.org/10.3390/polym16172421
28. Lafeuillee, C., Maharaj, R. (2025). A preliminary investigation of the properties of plantain starch-chitosan composite films containing Panadol leaf extracts. *Discover Food*, *5*(1). https://doi.org/10.1007/s44187-025-00270-4
29. Lau, W. N., Mohammadi Nafchi, A., Zargar, M., Rozalli, N. H. M., Mat Easa, A. (2024). Development and evaluation of Bauhinia Kockiana extract-incorporated sago starch intelligent film strips for real-time freshness monitoring of coconut milk. *International Journal of Biological Macromolecules*, *260*(P2), 129589. https://doi.org/10.1016/j.ijbiomac.2024.129589
30. Liyanapathiranage, A., Dassanayake, R. S., Gamage, A., Karri, R. R., Manamperi, A., Evon, P., Jayakodi, Y., Madhujith, T., Merah, O. (2023). Recent developments in edible films and coatings for fruits and vegetables. *Coatings 13*(7), 1177. https://doi.org/10.3390/coatings13071177
31. Mbonambi, N. P., Adeyemi, J. O., Seke, F., Fawole, O. A. (2025). Fabrication and application of bio-based natural polymer coating/film for food preservation: A review. *Processes 13*(8), 2436. https://doi.org/10.3390/pr13082436
32. Othman, S. H., Shapi'i, R. A., Ronzi, N. D. A. (2024). Starch biopolymer films containing chitosan nanoparticles: A review. *Carbohydrate Polymers*, *329*(December 2023), 121735. https://doi.org/10.1016/j.carbpol.2023.121735
33. Rachmina, R., Hasan, M., Hasanah, U., Halim, A. (2024). Sugar palm starch/chitosan bionanocomposite films incorporated with anthocyanin and curcumin – thermal properties and release kinetics. *Journal of Ecological Engineering*, *25*(2), 300–308. https://doi.org/10.12911/22998993/177140
34. Shamsuri, A. A., Md. Jamil, S. N. (2020). Functional properties of biopolymer-based films modified with surfactants: A brief review. In *Processes* 8(9), 1039. https://doi.org/10.3390/pr8091039
35. Souto, E. B., Yoshida, C., Leonardi, G., Cano, A., Sánchez-López, E., Zielińska, A., Viseras, C., Severino, P., Silva, C., De Melo Barbosa, R. (2021). Lipid-polymeric films: Composition, production and applications in wound healing and skin repair. *Pharmaceutics*, *13*, 1–23. https://doi.org/10.3390/pharmaceutics13081199
36. Tan, S. X., Ong, H. C., Andriyana, A., Lim, S., Pang, Y. L., Kusumo, F., Ngoh, G. C. (2022). Characterization and parametric study on mechanical properties enhancement in biodegradable chitosan-reinforced starch-based bioplastic film. *Polymers 14*(2), 278. https://doi.org/10.3390/polym14020278
37. Vostrejs, P., Adamcová, D., Vaverková, M. D., Enev, V., Kalina, M., Machovsky, M., Šourková, M., Marova, I., Kovalcik, A. (2020). Active biodegradable packaging films modified with grape seeds lignin. *RSC Advances*, *10*(49), 29202–29213. https://doi.org/10.1039/d0ra04074f
38. Wang, J., Sun, X., Zhang, H., Dong, M., Li, L., Zhangsun, H., Wang, L. (2022). Dual-functional intelligent gelatin based packaging film for maintaining and monitoring the shrimp freshness. *Food Hydrocolloids*, *124*(PA), 107258. https://doi.org/10.1016/j.foodhyd.2021.107258
39. Wang, N., Wei, J., Wang, C., Ren, J. (2025). Preparation, physicochemical properties, biological activity of a multifunctional composite film based on zein/citric acid loaded with grape seed extract and its application in solid lipid packaging. In *Foods 14*(10), 1698. https://doi.org/10.3390/foods14101698
40. Wattanawong, N., Aht-Ong, D. (2021). Antibacterial activity, thermal behavior, mechanical properties and biodegradability of silver zeolite/poly(butylene succinate) composite films. *Polymer Degradation and Stability*, *183*, 109459. https://doi.org/10.1016/j.polymdegradstab.2020.109459
41. Wibowo, A. H., Fehragucci, H., Purnawan, C. (2023). *ALCHEMY Jurnal Penelitian Kimia Effect of Plasticizer Addition on The Characteristics of Chitosan-Alginate Edible Film 1*. *19*(2), 123–129. https://doi.org/10.20961/alchemy.19.2.71348.123-129
42. Zhu, B., Zhong, Y., Wang, D., Deng, Y. (2023). Active and intelligent biodegradable packaging based on anthocyanins for preserving and monitoring protein-rich foods. *Foods*, *12*(24). https://doi.org/10.3390/foods12244491